

Life on Miller’s Planet: The Habitable Zone Around Supermassive Black Holes

Jeremy D. Schnittman

NASA Goddard Space Flight Center, Greenbelt, MD 20771

Joint Space-Science Institute, College Park, MD 20742

jeremy.schnittman@nasa.gov

ABSTRACT

In the science fiction film *Interstellar*, a band of intrepid astronauts sets out to explore a system of planets orbiting a supermassive black hole, searching for a world that may be conducive to hosting human life. While the film legitimately boasts a relatively high level of scientific accuracy, it is still restricted by Hollywood sensitivities and limitations. In this paper, we discuss a number of additional astrophysical effects that may be important in determining the (un)inhabitable environment of a planet orbiting close to a giant, accreting black hole. Foremost among these effects is the blueshift and beaming of incident radiation on the planet, due to the time dilation of an observer orbiting very close to the black hole. This results in high-energy flux incoming from surrounding stars and background radiation, with significant implications for habitability.

Subject headings: black hole physics – accretion disks – X-rays:binaries

1. INTRODUCTION

A favorite question in the popular discussion of black holes is, “what would happen if the sun were to suddenly turn into a black hole?” On the up side, we know that the Earth would not get “sucked in.” Far from a black hole (and the Earth is millions of Schwarzschild radii away from the Sun), gravity looks almost exactly Newtonian. On the down side, the Sun provides almost all the energy necessary for life on Earth to survive. Without its constant heat flux, the oceans would likely freeze over in a matter of days.

But we also know that many astrophysical black holes can provide their own energy source, in the form of radiation from hot, accreting gas. In fact, for most observable black

holes, this accretion power outweighs anything attainable from nuclear fusion by many orders of magnitude. So one could naturally imagine that replacing the Sun with an accreting black hole might not be the end of life on earth after all.

This entertaining thought experiment is not unlike the premise of the science fiction blockbuster *Interstellar*. The only difference is that, instead of replacing the Sun with a black hole, due to an imminent biological collapse on Earth, humanity is forced to leave the Solar System behind and seek out a new habitable world orbiting a distant black hole. **[Warning! Spoiler alert!]** Advanced probes have identified three potentially habitable planets orbiting a supermassive black hole called *Gargantua*. NASA then sends a follow-up team of astronauts and scientists to explore these three targets in detail, looking for more promising evidence for habitability.

In this paper, we ask the simple question: what could we know *a priori* about the environments of these planets, and in particular, the prospect of their habitability? On the face of it, this is nothing more than the typical armchair speculation and commentary disseminated by generations of sci-fi fans poking their fingers into any perceived plot hole. Yet we hope to show that the question of habitability around supermassive black hole is an extremely valuable pedagogical tool. Among the important physics problems involved are accretion dynamics, general relativity, tidal evolution, atmospheric chemistry, and astrobiology.

Many of these questions are already asked and answered in the movie’s excellent companion book *The Science of Interstellar* (Thorne 2014), a source on which we will naturally lean heavily. The primary novelty of this paper is the expanded discussion of habitability for exoplanets in general, along with a focus on the important implications of the extreme time dilation found on Miller’s planet.

It cannot be overemphasized that the purpose of this paper is *not* a critique of *Interstellar*, neither from the point of view of film quality or scientific accuracy. Rather, it should be understood as a form of fan fiction, exploring in greater detail and new directions the world created by Christopher Nolan and Kip Thorne.

2. DEFINITION OF HABITABILITY

We begin with the simple question of what makes a planet habitable? This is one of the most important and active areas of research in the exoplanet field today. Much like the multi-step triage strategy employed by the explorers in *Interstellar*, the NASA roadmap for exoplanet exploration involves a multi-stage approach where smaller probe missions (e.g., TESS, the Transiting Exoplanet Survey Satellite; Ricker et al. (2015)) are used

to identify promising targets for intense spectroscopic observations with the James Webb Space Telescope. Eventually, the goal is to find promising targets for direct imaging of Earth-like planets by future flagship missions such as the Large-aperture UV/O/IR Telescope.

These future direct imaging missions will ultimately have the goal of detecting biosignatures by identifying specific spectral features in the planet’s atmosphere. In the most plausible scenarios (in our admittedly limited, Earth-centric imagination), atmospheric biosignatures require the existence of liquid water on the planet’s surface. Thus, to first order, the *habitability zone* (HZ) for a planetary system is defined as the region where the equilibrium temperature on the planet’s surface is between 273 and 373 K.

To determine a planet’s equilibrium surface temperature, one simply balances the incoming heat sources with the outgoing radiative flux. Of course, in practice, this calculation can be anything but simple. For example, the total Solar flux incident on the Earth is 1250 W/m^2 . This flux is incident on a surface with cross sectional area πR_E^2 yet the radiated flux is emitted from an area of $4\pi R_E^2$. Assuming a blackbody emissivity law, the effective temperature can be solved from

$$4\pi R_E^2 \sigma T_{\text{eff}}^4 = \pi R_E^2 F_{\odot}, \quad (1)$$

giving $T_{\text{eff}} = 277 \text{ K}$. The actual value, averaged over the Earth’s surface, is $T_{\text{eff}} = 288 \text{ K}$.

It turns out that this close agreement is something of a happy coincidence, since we have ignored several important physical processes. First, not all of the solar radiation is actually absorbed by the Earth. Some is reflected off of clouds, icecaps, and even the ocean. This reflection is quantified by the *albedo* α , defined as the ratio of the reflected to incident flux. For the Earth, $\alpha \approx 0.3$, meaning only 70% of the incident solar radiation actually contributes to warming the surface. So we should simply modify equation (1) by multiplying the right-hand-side by $(1 - \alpha)$, giving an equilibrium temperature of 254 K, nearly 20 degrees below freezing!

However, the left-hand-side of (1) is also wrong, since not all the radiation emitted from the surface actually escapes to space. While the atmosphere is largely transparent to the incoming solar flux, which peaks at wavelengths around 400–600 nm, the outgoing infrared radiation ($\sim 10\text{--}15 \mu\text{m}$) is much easier to absorb in the atmosphere, specifically by molecules like H₂O, CO₂, and CH₄. This is the well-know “greenhouse effect,” which for Earth leads to a net warming of $\sim 34 \text{ K}$ over the simple equilibrium temperature, and gives us a warm, stable planet on which life can thrive.

What about other planets? Considering only solar system objects, the range of albedos on rocky bodies ranges from 0.1 for Mercury to 0.7 for cloud-covered Venus. Furthermore,

the magnitude of the greenhouse effect quoted above is only applicable for Earth’s present atmosphere and the Sun’s present spectrum. Changing either significantly could lead to vastly different figures. One need only look at Earth’s twin Venus to appreciate the potential implications of greenhouse warming. Largely motivated by Venus’s radically different climate, Kasting et al. (1993) employed a vertical 1D climate calculation with a detailed photochemical code so as to better understand the processes that could lead to a runaway greenhouse effect. They found that, as the incident solar flux or the mixing fraction of CO₂ increased above a critical value, the surface temperature would increase to the point where water vapor (a powerful greenhouse gas) would begin to dominate the atmosphere, further heating the planet until the oceans evaporated entirely. Once in the upper atmosphere, the H₂O could dissociate and the light H₂ could escape entirely, leaving a hot, dry, CO₂-dominated planet behind. Without liquid water, it becomes very difficult for the atmospheric CO₂ to get re-captured through weathering processes common on Earth, and thus accumulates in the atmosphere.

In the two decades since these early calculations, the 1D coupled climate-photochemistry codes have evolved significantly, incorporating more detailed opacity models as well as a more diverse range of chemical composition for the atmosphere. The current state-of-the-art results for the habitable zone can be found in Kopparapu et al. (2013), reproduced in Figure 1. The figure shows the “conservative” HZ as the region between the two blue curves, and the “optimistic” HZ between the red and orange curves.

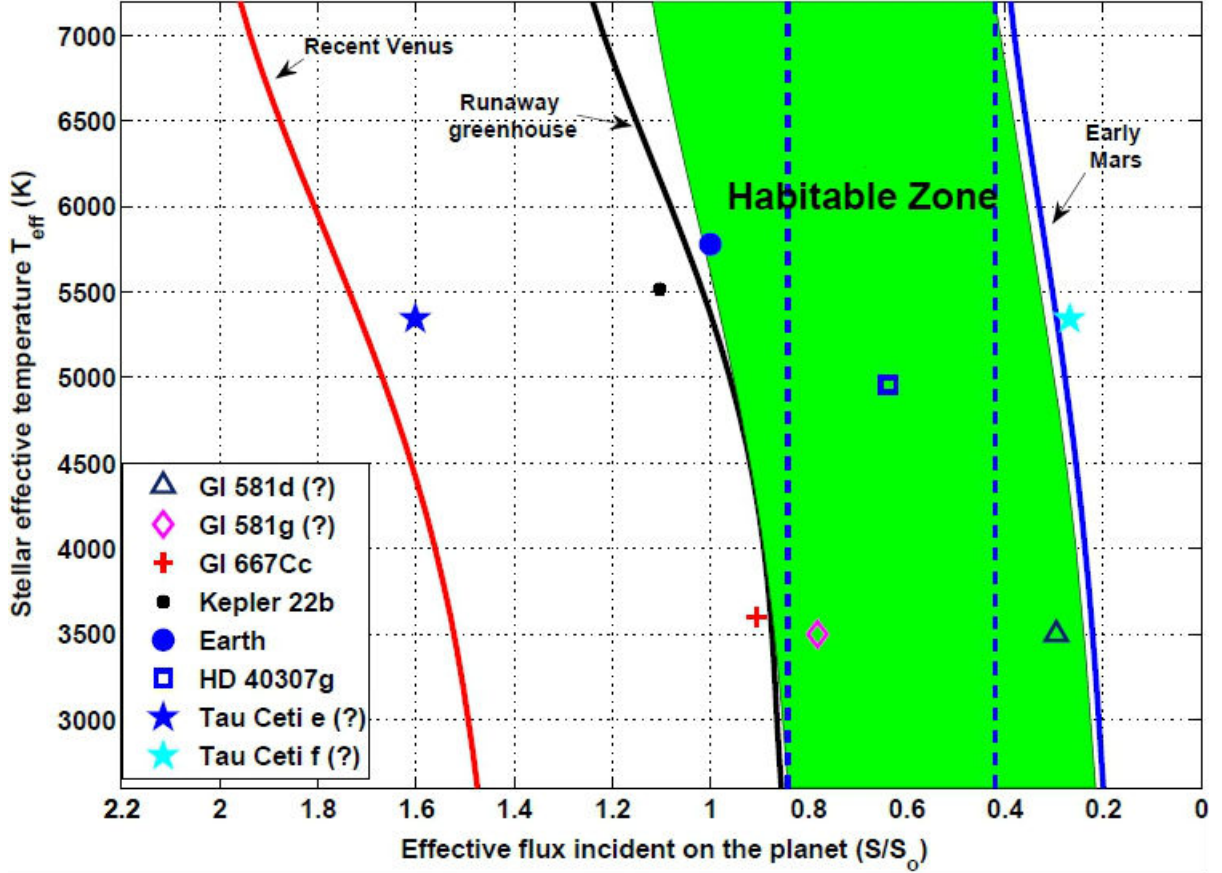
Somewhat ominously, the Earth is right at the inner edge of the conservative HZ, at clear risk of crossing the line to runaway greenhouse. Yet the calculations in Kopparapu et al. (2013) are only one-dimensional, and necessarily neglect many complicating factors such as cloud formation, which we will see below may have an important stabilizing effect on the climate.

We can also see in Figure 1 the effects of changing the host star’s mass, and thus the incident spectrum on the planet. Smaller stars are much less luminous, and also cooler, producing a blackbody spectrum peaking closer to the infrared. Thus the HZ for faint M-dwarf systems is well inside 0.1 AU.

Also plotted (dotted line) in Figure 1 is the tidal locking radius. Any terrestrial planet inside this point will likely be tidally locked to the host star on the timescale of a Gyr or less. Note that Mercury is just inside this line, consistent with the fact that it is quasi-locked to the Sun, trapped in a 3:2 spin-orbit resonance (Murray & Dermott 1999). In the Newtonian regime, the tidal forces are quite easy to calculate, and scale simply with the stellar mass to the one-third power:

$$R_{\text{tl}} \propto R_p (M_*/M_p)^{1/3} . \quad (2)$$

Fig. 1.— Habitable zone for planets with Earth-like atmospheres around a variety of stellar types. [reproduced with permission from Kopparapu et al. (2013)]



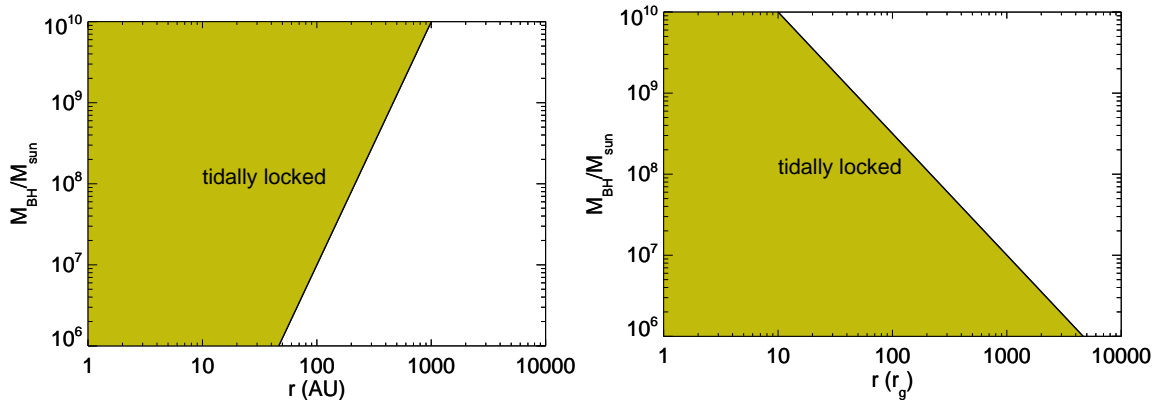
For rocky planets of similar composition and thus density, $R_p \sim M_p^{1/3}$ so the tidal locking radius R_{tl} is a function only of the stellar mass M_* .

Scaling equation (2) up to black hole masses naturally gives much larger tidal locking radii, as shown in Figure 2a. As in many studies of black holes, it is convenient to define the *gravitational radius* $r_g \equiv GM/c^2$ as a unit of length. This provides a valuable estimate for when relativistic effects become important, as first-order post-Newtonian corrections are proportional to $(v/c)^2 \sim (r/r_g)^{-1}$. Thus in Figure 2b we plot the tidal locking radius as a function of gravitational radii. This curve is determined simply by scaling up the Newtonian relationship to black hole masses. For black holes less than $\sim 10^9 M_{\odot}$, it seems likely that post-Newtonian effects will be unimportant on determining the specific tidal-locking radius. Above $10^9 M_{\odot}$, the relativistic form of the tidal tensor must be used, e.g., with locally flat

Fermi normal coordinates, as in Cheng & Evans (2013).

Much closer to the black hole (or more likely, for much smaller black holes), the gravitational forces could be so great as to tidally disrupt the planet. The tidal disruption radius R_{td} scales just like the locking radius R_{tl} , but roughly two hundred times smaller: $R_{\text{tl}} \approx 200R_{\text{td}}$. From Figure 2, we see that a terrestrial planet would get tidally disrupted just inside the horizon of Gargantua, making Miller’s planet deformed but not disrupted (Thorne 2014).

Fig. 2.— Tidal locking radius for rocky planets orbiting supermassive black holes as a function of black hole mass; the radius is measured in (a) astronomical units and (b) gravitational radii. Any planet inside R_{tl} will be tidally locked to the black hole.

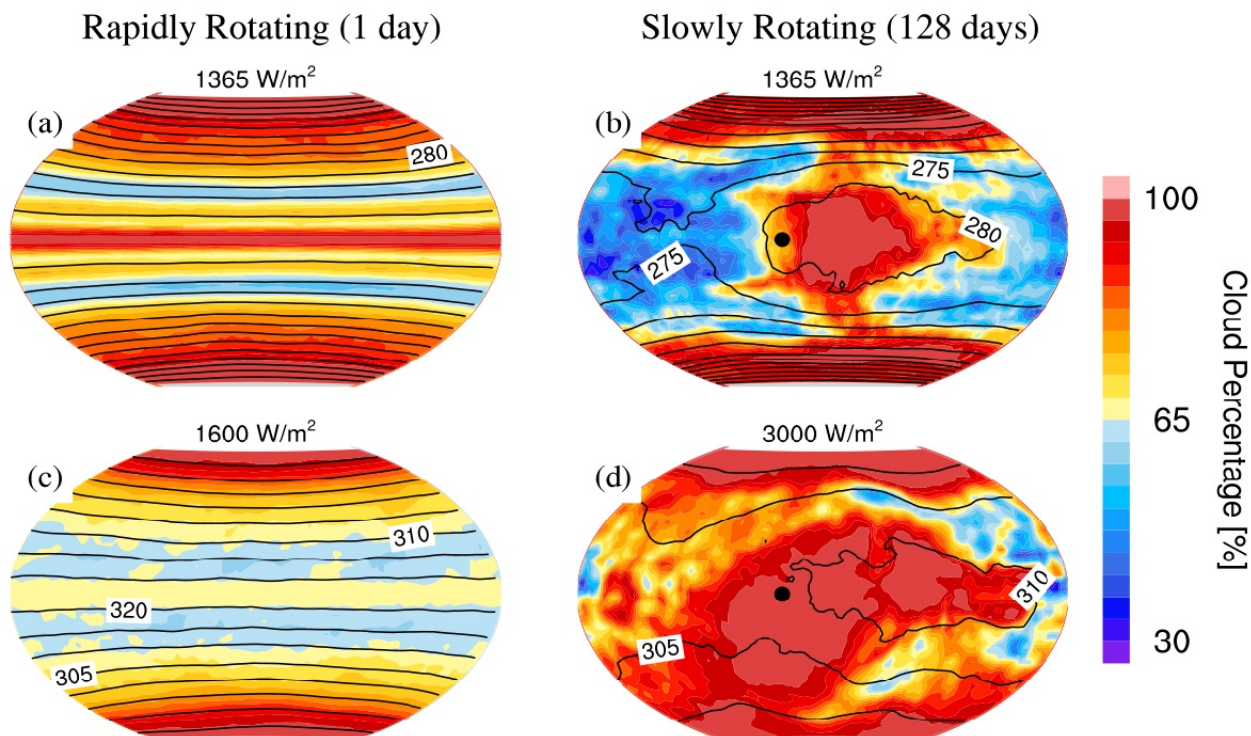


We can see from Figure 2 that for Gargantua’s mass of $10^8 M_{\odot}$ (Thorne 2014), any planet inside a radius of 100 AU will be tidally locked to the black hole. Conveniently enough, for this mass, one AU is almost exactly one r_g .

For tidally locked planets, the incoming flux is always absorbed at the same part of the planet. For planets around regular stars, this is called the “sub-stellar” point, directly facing the star. As we will see below, for planets around black holes, this will generally be a point facing in the direction of the planet’s orbit. In both cases, the absorbed flux must be transported around the planet via ocean or atmospheric currents, or else the dark half of the planet will freeze over.

Furthermore, the slow rotation of tidally locked planets will completely change the global circulation patterns that are familiar on rapidly-rotating planets like Earth. In particular, on Earth warm, moist air is heated around the equator, which then rises, cools, and forms a band of clouds and precipitation around the tropics. After releasing the bulk of its moisture near the equator, the resulting drier, cooler air flows towards the poles, eventually sinking in the sub-tropical arid latitudes around 30° (see Fig. 3a).

Fig. 3.— Cloud coverage maps with overlaid temperature contours for (left) rapidly and (right) slowly rotating planets. The strong cloud coverage at the sub-stellar point for tidally locked planets has a significant cooling effect on the surface temperature. [reproduced with permission from Yang et al. (2014)].



For tidally locked planets, instead of a band of rising air around the equator, there is more like a single stationary chimney at the sub-stellar point, lofting moisture in a pillar like a huge cumulonimbus cloud. This persistent cloud coverage acts like a sun shade, reflecting the vast majority of the incoming flux. To investigate this effect in detail, Yang et al. (2014) ran a full 3-D global circulation model (GCM) of an Earth-like planet with 1-day and 128-day rotation periods for a range of incoming flux. Even for (surface-integrated) fluxes as large as 750 W/m^2 , the mean surface temperatures of the slowly rotating planet was a balmy $32 \text{ }^\circ\text{C}$. Temperature contours and cloud coverage maps from their simulations are shown in Figure 3.

With these GCM results in hand, we will adapt an optimistically broad habitable zone for tidally locked planets, covering a range of incident flux ranging from 800 W/m^2 at the

inner edge, down to 120 W/m^2 at the outer edge. For planets outside the tidal locking orbit, we will still adopt a relatively optimistic inner edge to the HZ of 600 W/m^2 , corresponding roughly to the curve labeled “recent Venus” in Figure 1. This is based on empirical evidence that Venus has not had any surface water for at least the past Gyr (Solomon & Head 1991), so any Earth-like planet with comparable flux is likely uninhabitable. We will also assume that the energy balance is due only to bolometric flux. In other words, we assume the atmosphere is able to reprocess incoming flux over a wide range of wavelengths, although this will also certainly break down at a certain point.

3. Energy Sources

Now that we have defined the habitable zone in terms of a planet’s tidal properties and incident flux, the next step is to explore the range of potential energy sources for planets around supermassive black holes.

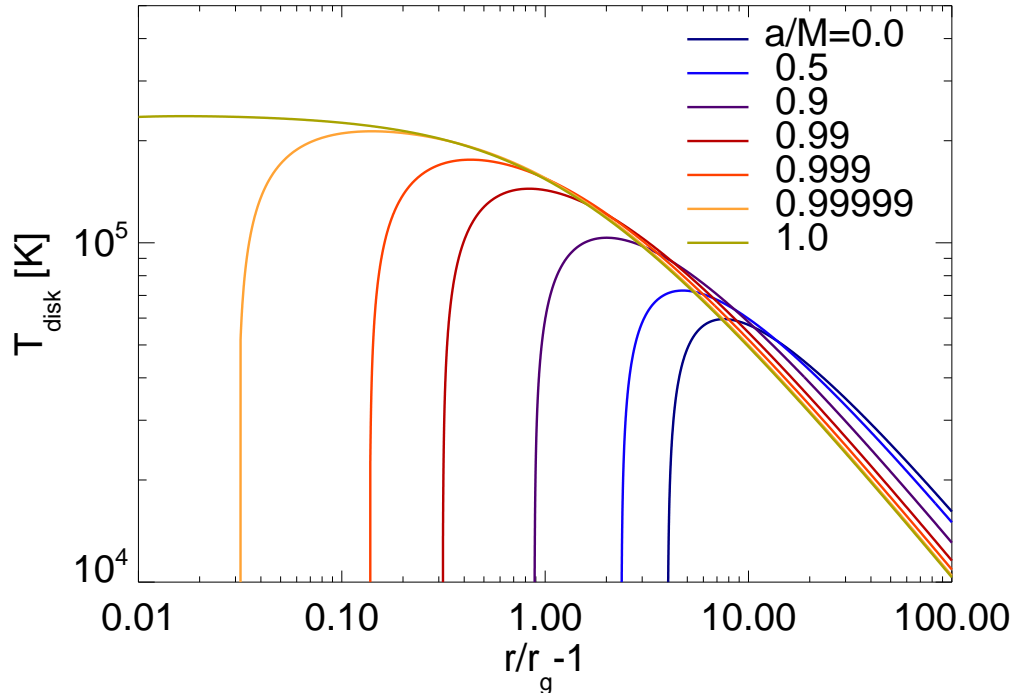
3.1. Accretion Disks

Most of what we know about black holes comes from observing the electromagnetic radiation coming from gas as it accretes onto the black hole. Accreting stellar-mass black holes are the brightest X-ray sources in the sky, and accreting supermassive black holes are the most luminous persistent sources in the universe. When the accretion rate is sufficiently high (probably above $\sim 10^{-2} \dot{M}_{\text{Edd}}$, with the Eddington rate defined as $\dot{M}_{\text{Edd}} \equiv L_{\text{Edd}}/(\eta c^2) \approx 10^{26} (M/10^8 M_{\odot}) \text{ g/s}$), the gas likely forms an optically thick, geometrically thin accretion disk.

Considering the motivation behind this paper, it only seems fitting to use the Novikov & Thorne (1973) model for accretion onto a Kerr black hole. Recent, more physical models based on magneto-hydrodynamic simulations differ mostly in the plunging region around black holes with low to moderate spin parameters (Schnittman et al. 2016). For Gargantua, with a spin of $a/M = 1 - 10^{-14}$, Novikov-Thorne should be quite sufficient. In the Novikov-Thorne accretion disk model, the gas moves on equatorial, circular geodesic orbits outside of the inner-most stable circular orbit (ISCO), and then plunges rapidly into the horizon. The local temperature of the gas increases with decreasing radius until it reaches a maximum a few r_g outside the ISCO, and then drops to zero at the ISCO.

In Figure 4 we plot the accretion disk temperature for a $10^8 M_{\odot}$ black hole accreting at 10% of the Eddington rate, for a range of spin parameters. Note the somewhat unusual

Fig. 4.— Local fluid temperature of Novikov-Thorne accretion disk around a $10^8 M_\odot$ black hole accreting at $0.1\dot{M}_{\text{Edd}}$.



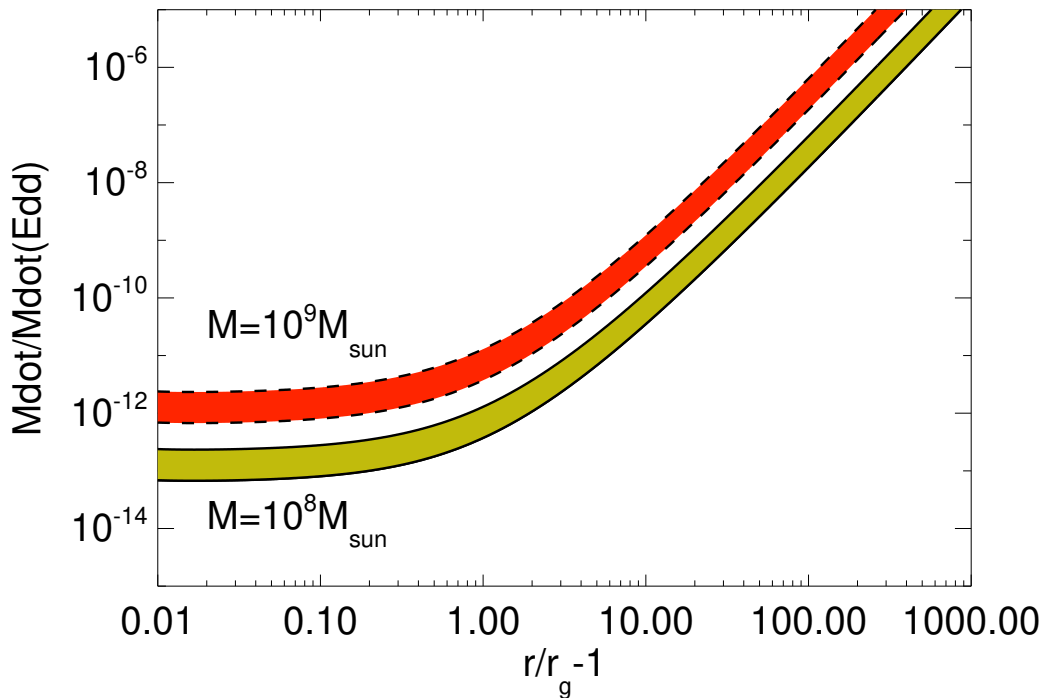
radial coordinates $r/r_g - 1$, which allow us to zoom in on the near-horizon region for nearly maximally spinning black holes. For these nominal parameters, we see that the peak temperature is around 10^5 K, consistent with the fact that most quasar spectra peak in the ultraviolet. The temperature scales with black hole mass and accretion rate like

$$T_{\text{peak}} \approx 2 \times 10^5 \left(\frac{M}{10^8 M_\odot} \right)^{-1/2} \left(\frac{\dot{M}}{0.1\dot{M}_{\text{Edd}}} \right)^{1/4} \text{ K}. \quad (3)$$

So if we want the accretion disk to look more like a main sequence star (indeed, the visualization of Gargantua’s accretion disk does appear a very similar color to our own Sun), we need to scale down the accretion rate by a factor of a million. Yet even after doing this, Miller’s planet, orbiting just outside the horizon, will be completely surrounded by a 6000-degree blackbody radiation field: hardly hospitable to life!

As seen in Figure 4, the disk temperature falls off with distance from the black hole, roughly as $T(r) \sim r^{-3/4}$. Thus a planet located at $\sim 100r_g$ should be immersed in a much more comfortable room-temperature bath of warm gas. This can be seen in Figure 5,

Fig. 5.— Habitable zone for planets embedded in a thin accretion disk around a Kerr black hole with $a/M = 1$ and mass $10^8 M_\odot$ (solid lines, yellow shading) and $10^9 M_\odot$ (dashed lines, red shading).



where we plot the extent of the HZ on the x-axis for a given accretion rate on the y-axis (alternatively, we can read this plot as saying, for a given semi-major axis, what range of accretion rates allow for habitability). In this scenario, we are using the HZ flux range of $120\text{-}600 \text{ W/m}^2$ even for the tidally locked regime, because a planet embedded in an optically thick accretion disk has not preferred direction from which the flux is greater, and thus dense cloud coverage will not be relevant to protecting the planet from stellar irradiation.

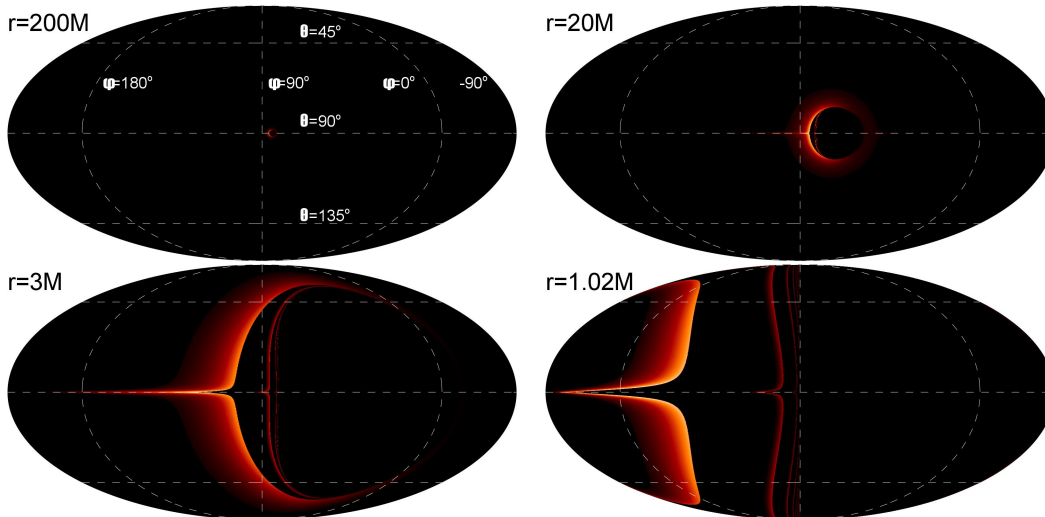
There are a couple problems with the results of Figure 5. First of all, if you were to immerse Earth in a bath of warm radiation at a temperature of 300 K, it would certainly be habitable according to our simple requirement of liquid water on the surface. However, all known life forms require an energy *gradient* in order to survive, so an all-pervasive blackbody radiation background would probably not be very conducive to complex life. Certainly not photosynthesis, which requires photon energies sufficient to break key molecular bonds.

The other, admittedly minor, problem with the embedded disk scenario is that, as clearly seen in the movie *Interstellar*, Miller’s planet is located outside the accretion disk. This is

somewhat surprising, and would be dynamically unlikely unless there were a sufficient gap in the disk, and the planet were endowed with some non-zero orbital inclination. Alternatively, we could imagine the accretion disk so geometrically thin that it just barely covered the planet’s equator, with the rest of the planet poking out above and below the disk. Indeed, according to the classical Novikov-Thorne model (Novikov & Thorne 1973), for the black hole masses accretion rates covered in Figure 5, the disk’s thickness would be on the order of a kilometer or less.

In this case, the incoming flux will not be limited to the local blackbody radiation from the disk, but will in fact include the entire view of the disk, as seen by an observer just above or below the surface. In Figure 6 we show what this disk might look like from the perspective of an observer at a few different distances from the black hole.

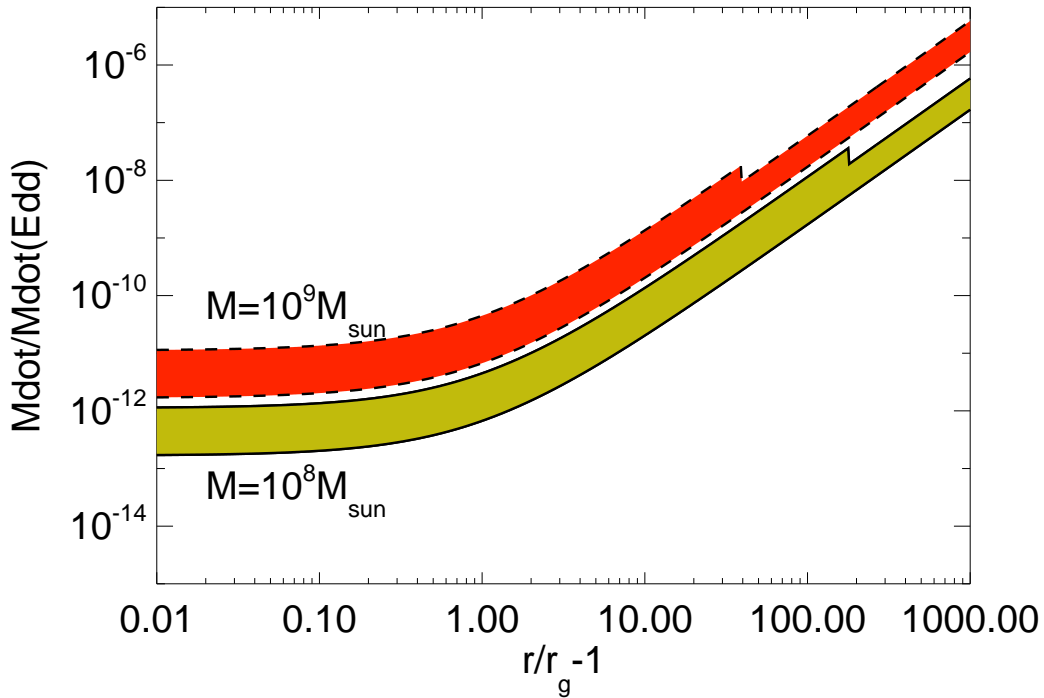
Fig. 6.— All-sky view of a thin accretion disk from an observer just above or below the disk. The black hole has spin $a/M = 1$ and the accretion disk extends from $r = 1M - 20M$ with a Novikov-Thorne emissivity profile. As the observer moves closer to the black hole, the disk and the horizon both fill a greater fraction of the sky, and multiple images are apparent, due to photons circling the black hole multiple times before reaching the observer.



The polar projections for these type of plots can be confusing. Consider the observer on a circular orbit in the black hole’s equatorial plane. The “forward” direction defines the $\phi = 0$ azimuth, and the θ angle is given by the standard spherical polar coordinates with “north” being $\theta = 0$ and “south” in the $\theta = \pi$ direction. This puts the black hole at $(\theta, \phi) = (\pi/2, \pi/2)$. Relativistic aberration shifts the apparent location of the black hole towards $\phi = 0$ as the observer moves to smaller radius.

Despite the fact that the observer is in the same plane as the accretion disk, and thus a razor-thin disk would in fact be invisible in Newtonian physics, the black hole’s gravity bends the trajectories of photons coming from the disk, making it appear as a ring (the “Einstein ring”) above and below the equatorial plane. In all cases in Figure 6, the disk is orbiting in the prograde direction around a maximally spinning black hole, so the approaching edge on the left side of each image will appear brighter due to relativistic beaming. Close to the black hole, multiple images of the disk become visible, due to photons that orbit the hole many times before eventually escaping and reaching the observer (James et al. 2015).

Fig. 7.— Habitable zone for planets just above or below a thin accretion disk around a Kerr black hole with $a/M = 1$ and mass $10^8 M_\odot$ (solid lines, yellow shading) and $10^9 M_\odot$ (dashed lines, red shading).



From $r = 200M$, the lensed accretion disk is roughly the same size of the Sun as viewed from the Earth. So if we set the accretion rate in order to match the apparent blackbody temperature of ~ 6000 K, the planet should be right in the middle of the HZ. This is exactly what we find, as shown in Figure 7, which is identical to Figure 5, only instead of the planet being embedded in the accretion disk, it is located just above or below the disk. Close to the black hole, this doesn’t make much difference, because the extreme gravitational lensing makes it look like much of the sky is subtended by the thermal disk. At larger radii, where

the local disk temperature is much colder, a planet outside of the disk will receive much more flux from the hot—yet distant—inner regions of the disk. Thus for a given accretion rate, the HZ moves out to larger radii relative to the embedded-in-disk paradigm. Also, because the flux is coming mostly from one specific direction, tidal locking will play an important role in determining habitability, as discussed above in Section 2. This can be seen clearly in Figure 7, which shows a broader HZ at smaller distances from the black hole, inside the tidal locking radius.

Regardless of the specific details—whether the planet is tidally locked or not, embedded in the disk or not—it is clear that for any planet to be habitable while also receiving its primary heating flux from a Novikov-Thorne type accretion disk, the planet either has to be extremely far from the black hole, or the mass accretion rate has to be an infinitesimal fraction of Eddington. This leads to an important inconsistency: The Novikov-Thorne model is predicated on an optically thick, radiatively efficient disk. At accretion rates down near $10^{-12}\dot{M}_{\text{Edd}}$, the optical depth is unlikely to be large enough to allow the gas to cool, thus leading to a very hot, low-density accretion flow.

3.2. Advective Accretion

Radiatively inefficient accretion flows (RIAF) encompass a large collection of more specific models, generally described by low densities, high temperatures, and large radial inflow velocities (Yuan & Narayan 2014). For simplicity, we adopt a collisionless, spherically symmetric inflow model as in Zeldovich & Novikov (1971). In this case, the density is given by

$$n(r) = n_0 \left(1 + \frac{2GM}{\sigma_0^2 r} \right)^{1/2}, \quad (4)$$

where n_0 and σ_0 are the density and velocity dispersion at large radius, respectively. The bulk velocity of the gas is given by the geodesic trajectory of a marginally bound particle falling from infinity with zero angular momentum (Schnittman 2015).

For a planet on a circular planar orbit in the black hole’s equatorial plane, the RIAF acts as a sort of “head wind” of low-density gas. We assume the kinetic energy of this gas is efficiently converted to heat in the planet’s atmosphere, providing the necessary heat for habitability. The center-of-mass energy of a single RIAF proton with 4-velocity u_1^μ hitting a proton in the planet’s atmosphere with 4-velocity u_2^ν is

$$E_{\text{com}} = m_p c^2 \sqrt{2(1 - g_{\mu\nu} u_1^\mu u_2^\nu)} \quad (5)$$

and the kinetic energy available for heat production is simply $E_k = E_{\text{com}} - 2m_p c^2$. Thus the

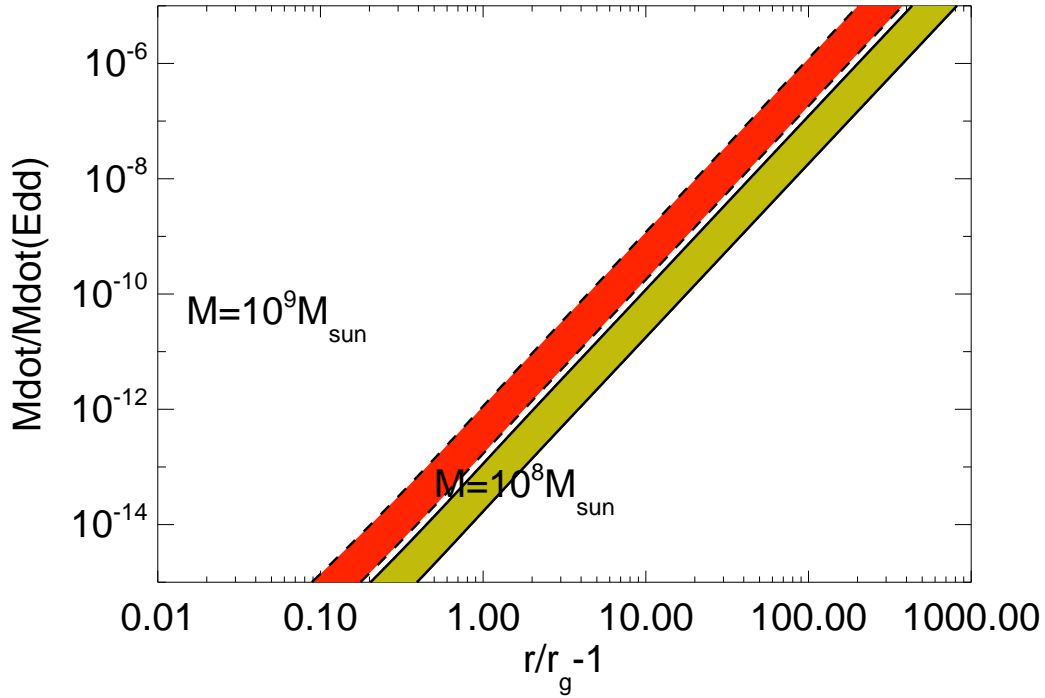
total incoming flux is

$$F = E_k n v, \quad (6)$$

with v the velocity of the planet relative to the accretion flow.

The density at a specific value of r/r_g scales like M^{-1} . This is because the total accretion rate is proportional to density times area, the accretion rate is proportional to the Eddington-scaled rate times the black hole mass, and the area is proportional to M^2 , so for a fixed Eddington-scaled rate, $\rho(r/r_g) \sim M^{-1}$.

Fig. 8.— Habitable zone for planets surrounded by a radiatively inefficient accretion flow around a Kerr black hole with $a/M = 1$ and mass $10^8 M_\odot$ (solid lines, yellow shading) and $10^9 M_\odot$ (dashed lines, red shading).



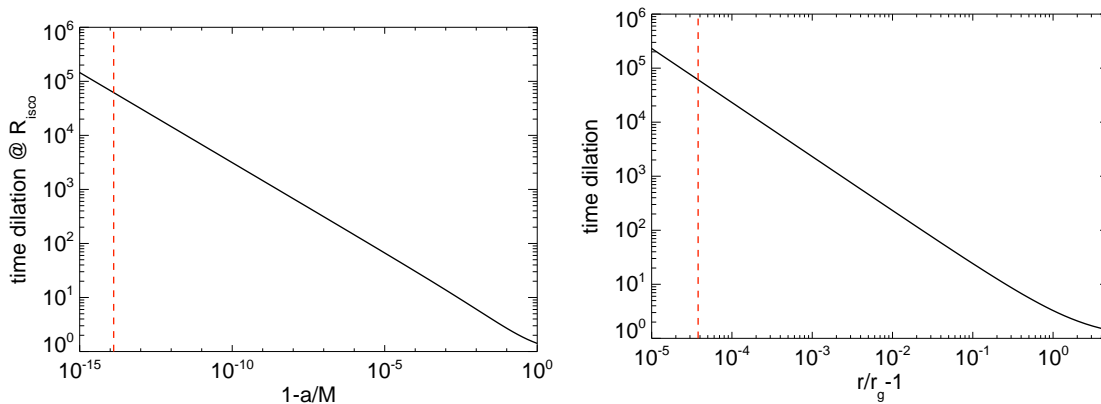
In Figure 8 we again plot the range of the HZ in terms of mass accretion rate and orbital radius for a Kerr black hole, now for a planet getting heated by the kinetic energy of incoming background gas. At large radius, the RIAF density is low and the relative velocity between the planet and the inflowing gas is small, so a higher net accretion rate is required in order to generate sufficient heat. As one approaches the horizon, the center-of-mass energy of incoming gas colliding with the planet’s atmosphere becomes so great, anything more than a tiny fraction of the Eddington accretion rate would be catastrophic for life on the planet.

For Miller’s planet, orbiting Gargantua at radius $r/M = 4 \times 10^{-5}$, the relativistic boost of incident particles would be a factor of nearly a thousand. Each gram of gas hitting the atmosphere would deliver the equivalent energy of 20 megatons of TNT!¹ Furthermore, as we will see in detail in the next section, the extreme time dilation near the black hole horizon will greatly increase the apparent rate at which the accreting gas is hitting the planet, making it even harder to achieve a habitable environment.

3.3. Background Radiation

Let us imagine, for argument’s sake, that there is in fact no accretion onto the black hole (clearly a deviation from the beautiful accretion disk images in *Interstellar*). In this case, what energy sources might a habitable planet avail itself of? Fortunately, everywhere you look in the Universe, there is a constant, steady stream of background radiation, most notably the cosmic microwave background (CMB). Shining at a cool 2.7 K, the CMB is hardly a promising source of radiation to keep a planet in the habitable zone.

Fig. 9.— Time dilation for an observer at the ISCO, as a function of black hole spin (*left*) and radius R_{ISCO} (*right*).



Yet this is where an important feature of relativity comes into play. As discussed extensively in the film, time slows down for observers close to a black hole. The time dilation on Miller’s planet is so extreme that one hour corresponds to seven years back on Earth (or even at the relatively nearby distance of Romily orbiting in the *Endurance* mother ship). Assuming the planet is on a stable, circular equatorial orbit, the minimum distance from the

¹See <http://what-if.xkcd.com/1/> for a discussion of a similar application to the game of baseball.

horizon is a strong function of black hole spin. As shown in Figure 9, Miller’s planet—with a time dilation factor of roughly 60,000—must be at a distance of no more than 4×10^{-5} gravitational radii outside the horizon, and thus the spin must be at least $a/M \gtrsim 1 - 10^{-14}$ (Thorne 2014).

Time dilation is directly related to redshift. Imagine Romily sending a Morse code message from the Endurance down to the surface of Miller’s planet. If he taps out one beep per second from his point of view, they will receive 60,000 beeps per second from their point of view! One can think of a photon as a type of clock, oscillating with a specific frequency². As that photon approaches the black hole, a local observer will measure a higher and higher frequency.

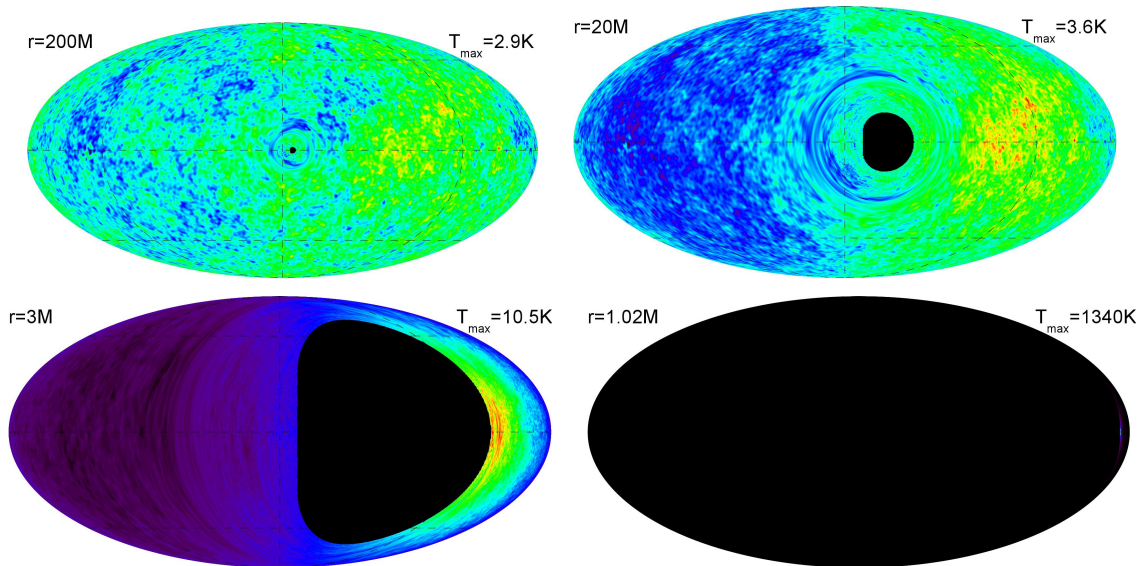
One of the nice things about blackbody spectra is that temperature is directly proportional to frequency, so if you Doppler-shift the entire spectrum to higher frequency, it remains a blackbody, only corresponding to a higher temperature. So for an observer orbiting a black hole, the blackbody CMB will still appear as a thermal spectrum, with temperature proportional to the blueshift in each direction. In Figure 10 we show what the CMB sky would look like to an observer orbiting a Kerr black hole at a few different radii. In each frame, the colors are chosen to cover the range of temperature from the minimum to maximum with a linear scale. We also intentionally use the standard WMAP color table, even though it counter-intuitively uses violet for low temperatures and red-orange for high temperatures.

Far from the black hole, the asymmetry is dominated by a simple dipole moment due to the orbital motion of the observer, just as in CMB sky maps made from Earth. We can also see the Einstein ring around the black hole, and the unique shadow of a Kerr black hole: an off-center truncated circle (Chandrasekhar 1983). Closer to the black hole, the size of the black hole shadow steadily increases until it fills half of the sky. Doppler and gravitational redshifts become more extreme, as does the relativistic beaming, effectively shrinking the size of the blue-shifted region, already only a few degrees across in the bottom-right panel of Figure 10.

At the same time, the solid angle of the hot spot decreases like the inverse square of the time dilation $dt/d\tau$, while the peak temperature approaches $T_{\text{peak}}/T_{\text{CMB}} = 9/2(dt/d\tau)$. These effects are shown in Figure 11, which zooms in on the area of peak CMB blueshift at orbital radii of $r = 1.0004M$ and $r = 1.00004M$ (the orbital distance of Miller’s planet from Gargantua).

²Indeed, this is exactly how atomic clocks work—connecting our standard of time to that of lasers tuned to specific atomic energy transitions.

Fig. 10.— All-sky view of the cosmic microwave background radiation, as seen from an observer orbiting in the equatorial plane of a Kerr black hole with spin $a/M = 1$. In each frame, the color scale is linear and covers a range from the lowest to highest observed CMB temperatures.

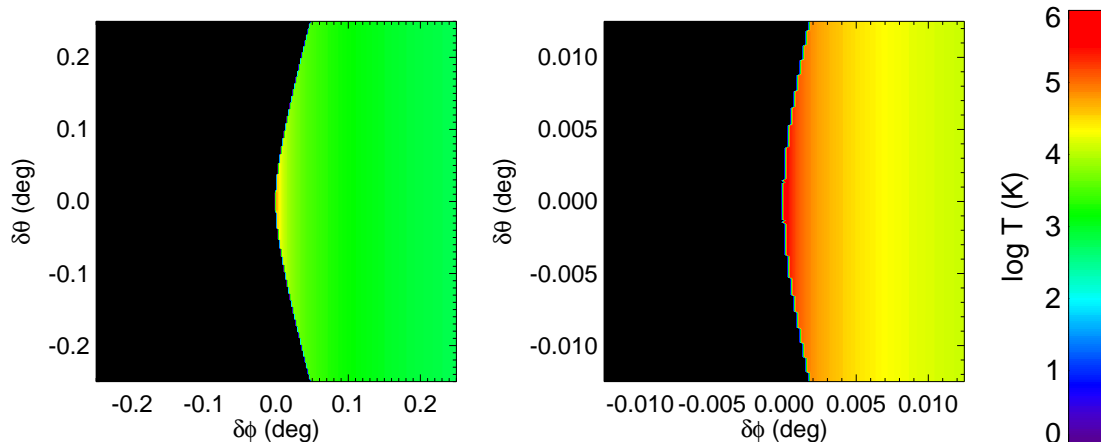


Thus the total incoming flux on the planet scales like $(dt/d\tau)^2 \sim (r - r_{\text{hor}})^{-2}$. When the background source is the isotropic CMB with a temperature of 2.7K, the habitable zone occurs around $r = 1.00036M$, where the incoming CMB has a temperature of 30,000K. This would be like orbiting a white dwarf at a distance of 0.2 AU. Perhaps the right temperature for liquid water, but with a lot of potentially lethal UV radiation.

At this radius, the planet’s time dilation relative to infinity would be a mere factor of 2,000. This would have the added advantage of giving the atmosphere and surface of the planet roughly five million years to cool and stabilize while the distant observer on Earth witnesses a Hubble time of cosmic evolution (Thorne 2014). On the other hand, an hour on the surface of this more habitable planet would only correspond to a few months for Romily in endurance, and Murph back home on Earth. Dramatic yes, but probably not enough to drive the plot of the movie.

In any case, this scenario of an idealized Earth-like environment at $r = 1.00036M$ is ignoring (at least) one crucial fact. While the CMB dominates the total electromagnetic energy density budget of the universe as a whole, there are localized regions in space where other backgrounds will certainly dominate. Near the Earth, the total flux in visible light

Fig. 11.— Zoom-in view of the region of greatest blueshift. In the left panel, the observer is at $r = 1.0004M$ and the zoom-in region is roughly the angular size of the Sun as seen from the Earth. On the right panel, the observer is on the same orbit as Miller’s planet ($r = 1.00004M$), with the CMB blueshifted to over 700,000K yet with an angular size comparable to Mars.



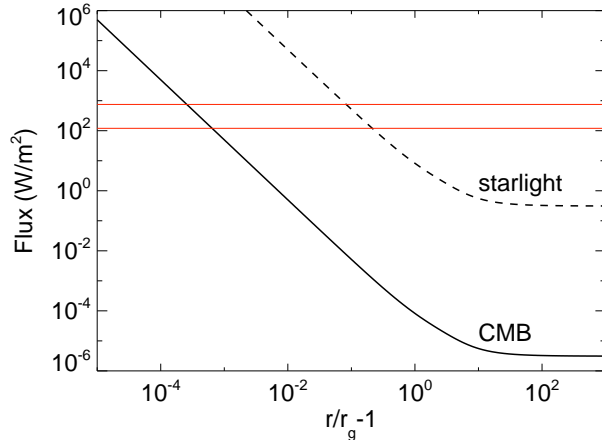
from nearby stars gives an effective background temperature of roughly 3K, coincidentally nearly equal to the CMB. Of course, this is only because we are situated in the middle of a galactic disk, where the local stellar density far exceeds that of the Universe on average.

For a planet orbiting a supermassive black hole situated in a galactic nucleus, the local stellar density will be orders of magnitude greater. For a planet in our own galactic center, the night sky would actually be 100,000 \times brighter than that of Earth! In Figure 12, we plot the mean flux on the planet’s surface as a function of distance from the BH horizon for $a/M = 1$. The habitable zone for a tidally locked planet is marked in red. Note that the HZ for planets irradiated by blueshifted starlight is at a relatively large radius of $1.1r_g$, where the time dilation is a measly factor of 23, but the blackbody temperature of a sun-like star would still be a whopping 600,000K. Again, technically habitable from an energy balance point of view, but challenging from a photochemical perspective.

3.4. Neutrinos

Perhaps a civilization that is sufficiently technologically advanced will be able to construct a sort of “reverse Dyson sphere” surrounding their planet with highly reflective material, effectively raising the planet’s albedo to near unity. This would allow habitability

Fig. 12.— Radiation flux incident on a planet orbiting an extremal Kerr black hole, due to blue-shifted background radiation from the CMB (solid curve) or ambient starlight in the galactic center (dashed curve). The HZ flux range is marked by the horizontal red lines.



much closer to the host SMBH, even in the face of overwhelming background UV or X-ray radiation.

Yet even with such a protective shield, there is still the specter of nature’s silent killer: neutrinos. From a simple calculation of thermal equilibrium during the early expansion after the big bang, one can determine that a cosmic neutrino background freezes out at temperatures of roughly 2.5 MeV. As relativistic particles, the neutrinos cooled exactly like the photons during the expansion, but the photons received the added energy stored in the electron-positron plasma that annihilated around temperature 0.5 MeV. Thus the subsequent radiation background is slightly hotter than the primordial neutrino background. While the CMB has a blackbody temperature of 2.73 K, the $C\nu B$ has $T = 1.95$ K (Weinberg 2008). While this background has not yet been detected directly, it has been indirectly inferred from the CMB measurements with Planck (Planck Collaboration et al. 2016).

Of course, the much more important difference between the neutrino and photon backgrounds is that the neutrinos have a very small cross section, so most go right through the atmosphere without depositing any energy. A reasonably good estimate for the neutrino-baryon cross section can be approximated by

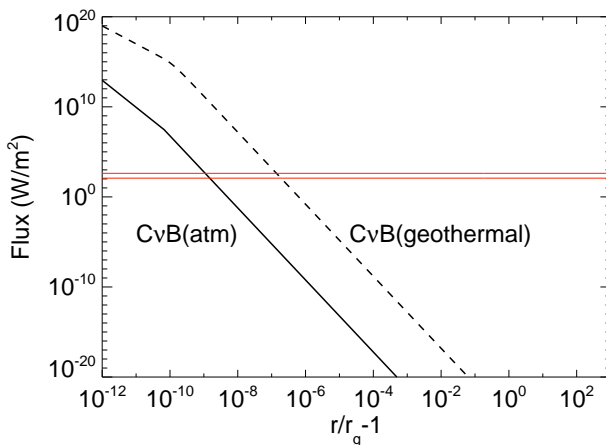
$$\sigma_\nu \approx 9 \times 10^{-44} \text{cm}^2 \left(\frac{E}{\text{MeV}} \right)^2 \quad (7)$$

for neutrino energies below 100 MeV, and

$$\sigma_\nu \approx 7 \times 10^{-42} \text{cm}^2 \left(\frac{E}{\text{MeV}} \right) \quad (8)$$

at higher energies.

Fig. 13.— Neutrino flux absorbed by the atmosphere (solid line) or body (dashed line) of an Earth-like planet orbiting an extremal Kerr black hole, due to blue-shifted cosmic neutrino background ($C\nu B$).

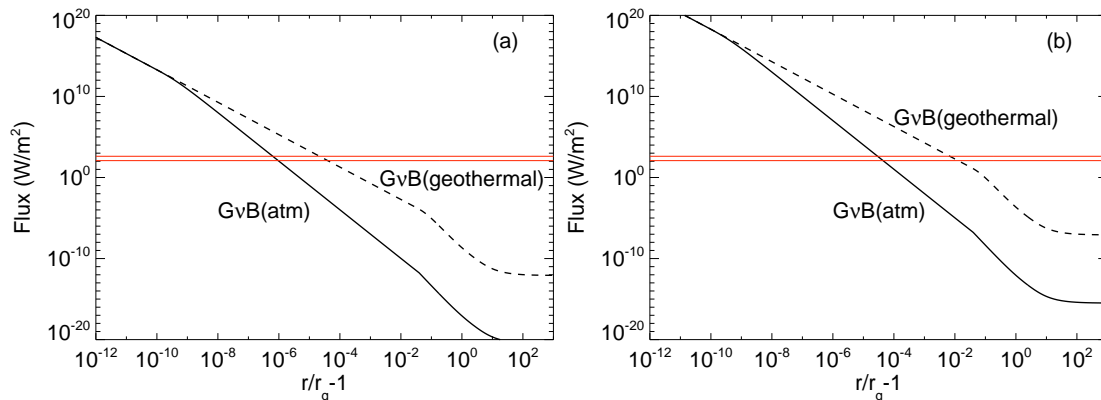


The blue-shifted $C\nu B$ flux is shown in Figure 13 as a function of radius. Note the vastly expanded axes relative to Figure 12. Only at a blueshift of roughly 10 billion does the $C\nu B$ deposit enough energy in the atmosphere to keep a planet within the habitable zone (designated by the horizontal red lines, as in Fig. 12). Yet many of the neutrinos that pass right through the atmosphere are subsequently absorbed in the dense core of the planet, so this energy could also be harnessed for heating up the surface for life. In that case, the required blueshift for habitability is 100 times smaller (dashed line in Fig. 13). Note the bends in the flux curves around $r/r_g = 1 + 10^{-10}$ correspond to the point where the typical $C\nu B$ energy rises above 100 MeV, where the cross section scaling changes. It coincidentally also corresponds to the point where the planet’s body becomes optically thick to neutrinos, and thus the absorbed flux doesn’t rise as much with increasing energy and cross section, giving a slightly flatter curve than that of the flux absorbed in the atmosphere.

On Earth, the $C\nu B$ flux (incident, not absorbed) is slightly smaller than that of the CMB, with a total flux of $8 \times 10^{-7} \text{ W/m}^2$. On the other hand, the solar neutrino flux is a whopping 40 W/m^2 , and these neutrinos have much higher energies—typically 0.1 – 10 MeV, giving much higher cross sections. Of course, a planet like Miller’s planet won’t have

a nearby star bathing it in neutrinos from nuclear reactions. In the interstellar medium, the dominant source of high-energy neutrinos is the background population of old supernova remnants (SNRs), contributing roughly 10^{-8} W/m² of neutrinos with energies of 10 MeV and above (Sigl 2012). We refer to this source as the Galactic neutrino background (G ν B).

Fig. 14.— Neutrino flux absorbed by the atmosphere (solid line) or body (dashed line) of an Earth-like planet orbiting an extremal Kerr black hole, due to galactic background neutrinos. In panel (a) we show flux corresponding to Solar System environments, while (b) is appropriate for a galactic center with flux roughly 10^5 times higher.



As shown in Figure 14, when blueshifted to higher energies and cross-sections, this G ν R neutrino flux reaches habitability levels at $r/r_g - 1 = 10^{-6}$ and 3×10^{-4} for atmospheric and planetary absorption, respectively. For these neutrinos, even the atmosphere is optically thick at sufficiently high blueshift, corresponding to PeV energies. Lastly, we note that, just like the background starlight, the SNR neutrino background is expected to be roughly 10^5 times greater near the galactic center. These enhanced fluxes are shown in panel (b) of Figure 14. Remarkably, the subsequent geothermal heating from neutrinos is only a factor of 100 below that of the background starlight. And unlike the harmful UV or X-ray flux from this blueshifted electromagnetic radiation, neutrino heating of the planet’s core could lead to a thriving population of lifeforms similar to those found near deep ocean vents on Earth.

3.5. Dark Matter

Neutrinos aren’t the only pervasive, invisible source of energy in the Universe. There is also dark matter, which actually makes up significantly more of the universe by mass (27% for dark matter, vs 0.003% for neutrinos), but is even more difficult to detect. One of the

leading models for dark matter is that of WIMPs: weakly interacting massive particles. Here “weakly” is a technical term, not just an adjective. It means the invisible particles interact with regular matter via the weak nuclear force, similar to neutrinos. And by “massive,” we really only mean that the rest mass is much greater than the energy, as opposed to neutrinos, which are thought to have a tiny rest mass, and thus their energy is dominated by their relativistic velocity.

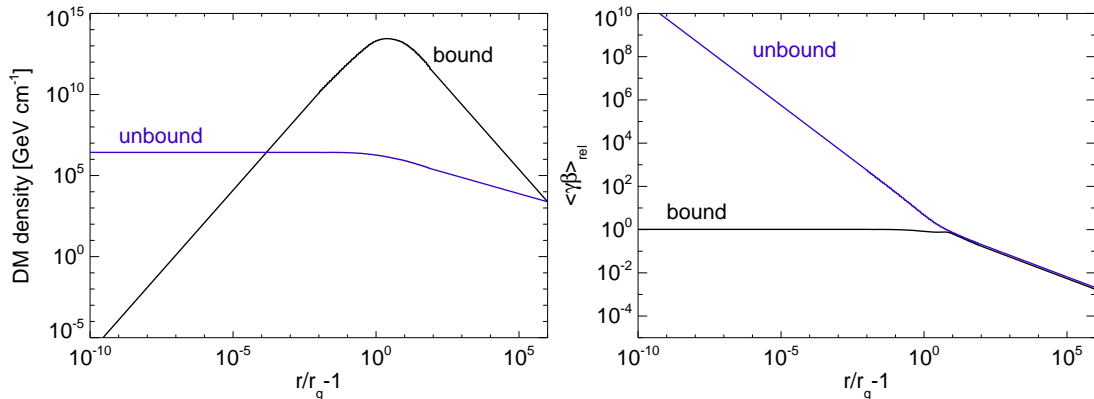
Most WIMP searches have focused on the GeV-TeV mass scales, so roughly on the order of typical atomic nuclei. This means that the number density of WIMPs in the solar neighborhood is actually much smaller than that of neutrinos, roughly 10^{-3} cm^{-3} vs $\sim 100 \text{ cm}^{-3}$ for the neutrinos. Furthermore, because the dark matter (DM) is cold, the kinetic energy density due to the random motion of the DM particles (typically $\sim 100 \text{ km s}^{-1}$ in the solar neighborhood) is also small, on the order of a few eV cm^{-3} . In order to be a viable heating source, we need a much higher concentration of much higher energy DM particles.

Fortunately, rapidly spinning SMBHs can provide both! After all, just about the only thing we know for sure about dark matter is that it interacts with gravity. What better tool could be imagined for accelerating dark matter than a gravity engine like a black hole? As we’ve seen multiple times in the previous sections, the extreme blueshifts experienced close to the event horizon can transform insignificant background radiation into a powerful energy source for sustaining (or destroying) life on a planet very close to the black hole. The same goes for dark matter, although now there is an added effect due to the gravitational focusing of the DM particles by the BH. As described in Schnittman (2015), we can treat the DM as made up of two distinct populations: the bound, and unbound particles. The unbound particles essentially plunge in towards the BH from far away, and have total energy close to their rest mass energy. Here, “far away” means just outside the BH influence radius, where the velocity dispersion of the ambient stars, gas, and DM is dominated by the overall gravitational potential of the galactic nucleus, not the black hole. In practice, this is typically on the order of parsecs for SMBHs with masses of $\sim 10^8 M_\odot$, or $200,000 r_g$.

For the unbound population, the gravitational focusing is a relatively weak effect, leading to a density profile scaling like $\rho \sim r^{-1/2}$ (Schnittman 2015). On the other hand, over hundreds of millions of years, as the SMBH grows through accretion, orbiting DM particles can get adiabatically trapped on closer and closer orbits, leading to a steep density cusp around the black hole (Gondolo & Silk 1999; Sadeghian et al. 2013; Ferrer et al. 2017), with the density scaling like $\rho \sim r^{-2}$. This bound population has negative binding energy, and is also limited to stable geodesic orbits, so cannot sample the full range of phase space as the unbound population.

Combining the two effects (gravitational focusing, and random orbital motion), in Figure

Fig. 15.— Dark matter distribution around a Kerr black hole. The DM density, as measured by an observer on a circular, equatorial orbit, is plotted in panel (a). In (b) we show the average value of $\beta\gamma$ for the DM particles incident on the observer. In both plots we show the bound and unbound DM populations, as described in the text.

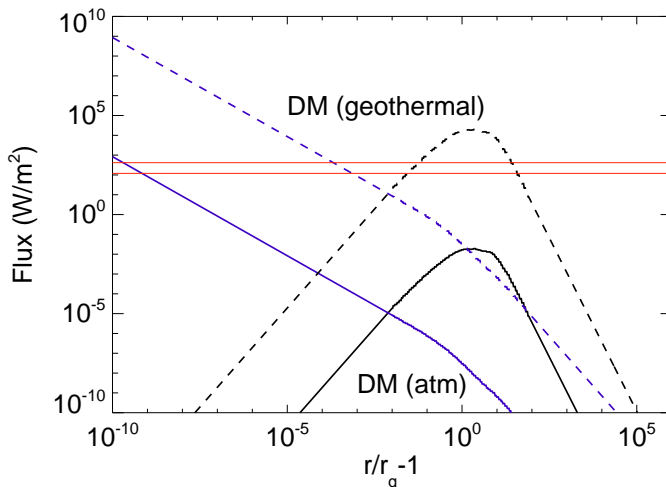


15 we show the density and mean relative velocity between DM particles as a function of distance from an extremal Kerr black hole. At large radius, the populations blend into a single population, but closer to the black hole we see the bound population’s density rise sharply to a peak a few r_g from the horizon, then decrease sharply as fewer and fewer stable orbits are available. These stable orbits are very nearly circular, pro-grade, equatorial orbits, so the relative velocity is constant. For the unbound particles, however, almost any random trajectory can be reached, leading to extremely high relative velocities. In fact, for perfectly extremal black holes, the center-of-mass energy between plunging particles can grow without bound as the trajectories approach the horizon (Bañados et al. 2009; Schnittman 2014).

To calculate the heating rate due to DM interactions with a planet, we need to estimate the cross section of DM-baryon scattering. Since dark matter has still not been directly detected, we are forced to use the latest upper limits from underground experiments. We adopt a generous cross section of $\sigma_{\text{WIMP-baryon}} \approx 10^{-41} \text{ cm}^{-2}$ for $m_\chi = 10 \text{ GeV}$, based on the results from the CDMS run in 2015 (Agnese 2016), and consistent with other similar underground experiments. Of course, we really have no idea what the actual cross section might be, or how it might scale with energy, or how the energy coupling mechanism might work, but as with the rest of this paper, we take our best guess, and follow the equations where they lead (and beyond).

In Figure 16 we show the energy flux incident on an Earth-like planet due to WIMP-baryon scattering in the atmosphere (solid lines) and in the interior of the planet (dashed

Fig. 16.— Flux on a planet due to scattering of dark matter particles off nucleons in the atmosphere (solid lines) or the planet’s interior (dashed lines). As in Figure 15, we consider both the bound (black lines) and unbound (blue lines) dark matter population.



lines). Outside of $r = 1.01r_g$, the flux is dominated by the bound population, where the enhanced density compensates for the lower energy particles. In fact, the density would be so great as to make the planet uninhabitable except for two narrow bands at $r \approx 1.03r_g$ and $r \approx 30r_g$. This is a remarkably distant habitable zone for such a weak (yet admittedly speculative) energy source.

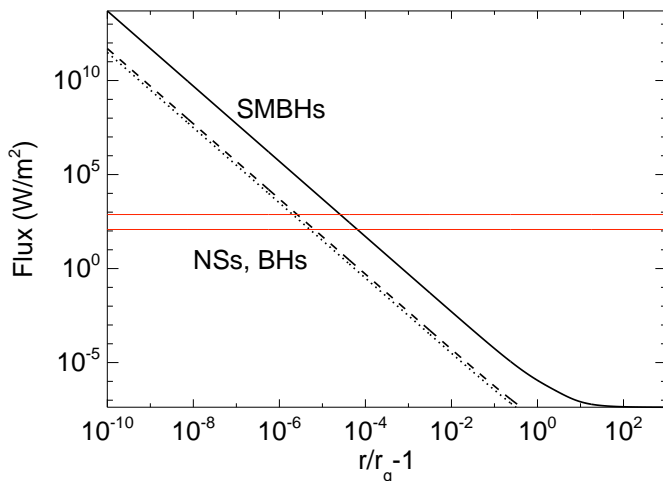
We should point out that the very existence of a bound population of DM and its accompanying density cusp is as-yet unproven. On much firmer ground is the unbound population, which certainly exists down to near the influence radius. And as long as there is dark matter near the influence radius, the gravity of the black hole will certainly focus and accelerate it as in Figure 15. In this case, the unbound population leads to very high energy collisions inside of $1.01r_g$, and habitable energy levels around $1.0003r_g$, still well outside of the nominal orbit for Miller’s planet.

3.6. Gravitational Waves

According to Kip Thorne, an early version of the screenplay for *Interstellar* involved the discovery of the wormhole to Gargantua through the detection of anomalously strong gravitational waves (Thorne 2014). Thus we find it fitting to conclude this exploration by imagining the interaction of gravitational waves (GWs) with a planet around a SMBH,

combining the two most amazing pieces of Einstein’s “outrageous legacy” (Thorne 1994). Ironically, Thorne’s version of the story has LIGO detecting the GWs from a neutron-star/black hole merger in 2019, which may very well be the year that the first such event was detected. In “real life,” LIGO’s first detection came just over a year after the release of *Interstellar*, in September 2015.

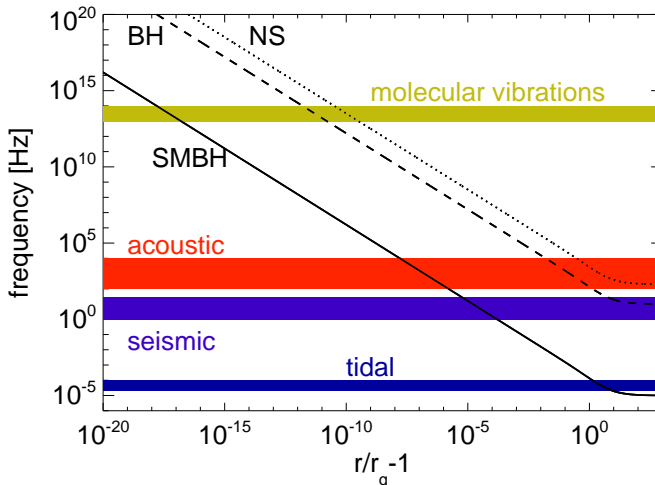
Fig. 17.— Flux on a planet due to gravitational waves from a stochastic population of neutron stars (dotted lines), stellar-mass BHs (dashed), and SMBH binaries (solid), as a function of orbital radius.



To date (halfway through LIGO’s O3 observing run), over thirty BH-BH mergers have been detected, as well as a handful of NS-NS events. From these initial detections, we can estimate the event rates in the local(ish) Universe to be $30 \text{ Gpc}^{-3} \text{ yr}^{-1}$ for the fiducial $30+30M_{\odot}$ systems like GW150914, and $600 \text{ Gpc}^{-3} \text{ yr}^{-1}$ for NS-NS mergers like GW170817 (The LIGO Scientific Collaboration & the Virgo Collaboration 2018). For simplicity, we further assume that all the energy is released at a single frequency: 5% of the rest mass for BH-BH, at 150 Hz, and 1% of the rest mass for NS-NS, at 3 kHz. This leads to a steady-state flux of GWs throughout the universe of roughly $6 \times 10^{-12} \text{ W m}^{-2}$.

We may as well add to this the flux from SMBH binary mergers, whose rates are not well constrained, but one reasonable estimate is that each Milky Way-type galaxy undergoes one major merger during its lifetime. The SMBH density at $z = 0$ is roughly $10^6 M_{\odot} \text{ Mpc}^{-3}$ (Li et al. 2011), dominated by black holes in the $10^{7-8} M_{\odot}$ range. This gives a merger rate of $10^{-3} \text{ Gpc}^{-3} \text{ yr}^{-1}$, or a flux of 10^{-8} W m^{-2} , peaked around 0.045 mHz. The flux in a gravitational wave is proportional to \dot{h}^2 , the derivative of the strain amplitude squared, so the observed flux scales like the GW frequency squared. Thus the same blueshifting effects

Fig. 18.— Flux on a planet due to gravitational waves from a stochastic population of neutron stars (dotted lines), stellar-mass BHs (dashed), and SMBH binaries (solid), as a function of orbital radius.



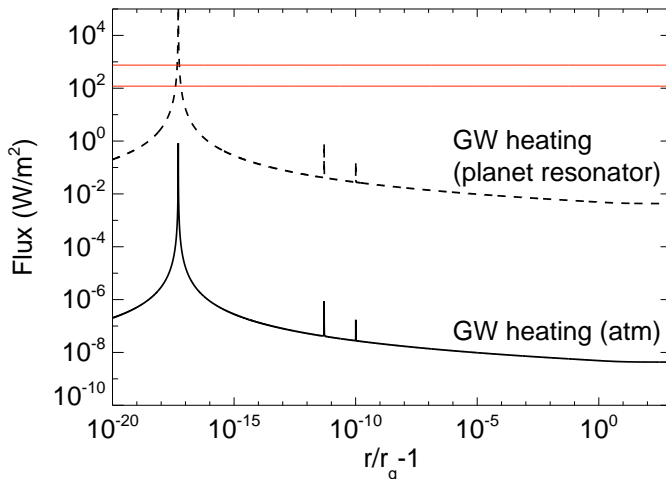
so important to electromagnetic radiation will also amplify the GW flux seen by a planet near the black hole horizon.

In Figure 17 we plot the GW flux due to stellar-mass BHs and NSs, as well as SMBHs, which turn out to dominate the background. As before, we mark the narrow band of habitability, corresponding to $r \approx 1.00003r_g$, right around the location of Miller’s planet! However, we have not discussed how this GW power might actually couple to the planet to provide a viable heating source. Gravitational waves are notoriously bad at coupling to matter, which is why it took a century between their prediction and detection.

In Figure 18, we consider a few conceivable physical coupling mechanisms between the GW background and the planet. Again, note the expanded x-axis, required to cover the huge dynamic range of physical processes under consideration. At the lowest frequencies are tidal forces, operating on the timescales of hours (just like in Miller’s planet! Thorne (2014)). At somewhat higher frequencies, global seismic modes (1-10 Hz) or mechanical acoustic vibrations (100-2000 Hz) become important. Here, the GWs could make the planet hum quietly, but still lack the necessary power to do any significant work. At much higher frequencies, we reach the band of molecular vibrations, coinciding with infrared absorption bands in the 10^{13-14} Hz range. Ironically, this brings us full-circle to our initial discussion of habitability and energy absorption in Earth-like atmospheres. Except now, the molecules would be excited by gravitational, not electromagnetic radiation.

Like EM radiation, we imagine the coupling will be most efficient near resonant transitions. For argument sake, we take the typical molecular vibration bands to centered at $10^{13.5}$ Hz, and treat the molecule like a mechanical ball-and-spring toy model, physically driven by the gravitational waves, and with a resonance width of $\delta\omega/\omega_0 = 10^{-3}$. Then the power delivered to the resonator is given by a Lorentzian function, just like a classical damped, driven harmonic oscillator. Again, we consider absorption in both the atmosphere, and interior of the planet.

Fig. 19.— Absorbed flux on a planet due to gravitational waves from a stochastic population of neutron stars, stellar-mass BHs, and SMBH binaries, as a function of orbital radius. The flux is absorbed via molecular vibrations in the atmosphere (solid curve) or the planet interior (dashed curve).



Combining the three source classes, the absorbed power is plotted in Figure 19. We are left with a single, precariously narrow band of habitability at $r/r_g - 1 \approx 5 \times 10^{-18}$. As with most of the other energy sources considered in this paper, resonant molecular heating from GWs would likely be extremely unpleasant to experience, as the very fabric of our existence would be shaken to its very core.

4. Discussion

In this paper, we have explored the possibility of a habitable Earth-like planet in orbit around a supermassive black hole. At times tongue-in-cheek, and at times fantastical, we nonetheless found the study informative, and a useful pedagogical tool for introducing

students (and professionals) to a wide range of fascinating astrophysical topics.

Just like in the movie *Interstellar*, the best science fiction stories are the ones that can push us to test the limits of our own scientific understanding, especially in the extreme cases found around black holes. As we have seen, it is not just the irreversible nature of the black hole’s event horizon that can drive the narrative of a science fiction story, but the bizarre effects that gravity has on time and trajectories of particles and light. For ultimately, what is narrative, if not the description of our own passage through time and space?

Acknowledgments

This work was inspired and motivated by the film *Interstellar*, directed by Christopher Nolan and advised by Kip Thorne. We gratefully acknowledge support from the Goddard Interdisciplinary Science Task Group program initiated by Piers Sellers. Zachary Shrier provided invaluable comments and discussion of the film and paper.

REFERENCES

- Agnese, R. e. a. 2016, *Phys. Rev. Lett.*, 116, 071301
- Bañados, M., Silk, J., & West, S. M. 2009, *Physical Review Letters*, 103, 111102
- Chandrasekhar, S. 1983, *The mathematical theory of black holes*
- Cheng, R. M., & Evans, C. R. 2013, *Phys. Rev. D*, 87, 104010
- Ferrer, F., Medeiros da Rosa, A., & Will, C. M. 2017, *Phys. Rev. D*, 96, 083014
- Gondolo, P., & Silk, J. 1999, *Physical Review Letters*, 83, 1719
- James, O., von Tunzelmann, E., Franklin, P., & Thorne, K. S. 2015, *Classical and Quantum Gravity*, 32, 065001
- Kasting, J. F., Whitmire, D. P., & Reynolds, R. T. 1993, *Icarus*, 101, 108
- Kopparapu, R. K., Ramirez, R., Kasting, J. F., et al. 2013, *ApJ*, 765, 131
- Li, Y.-R., Ho, L. C., & Wang, J.-M. 2011, *ApJ*, 742, 33
- Murray, C. D., & Dermott, S. F. 1999, *Solar system dynamics* (Cambridge University Press)
- Novikov, I. D., & Thorne, K. S. 1973, in *Black Holes (Les Astres Occlus)*, ed. C. Dewitt & B. S. Dewitt, 343–450
- Planck Collaboration, Ade, P. A. R., Aghanim, N., et al. 2016, *A&A*, 594, A13
- Ricker, G. R., Winn, J. N., Vanderspek, R., et al. 2015, *Journal of Astronomical Telescopes, Instruments, and Systems*, 1, 014003
- Sadeghian, L., Ferrer, F., & Will, C. M. 2013, *Phys. Rev. D*, 88, 063522
- Schnittman, J. D. 2014, *Physical Review Letters*, 113, 261102
- . 2015, *ApJ*, 806, 264
- Schnittman, J. D., Krolik, J. H., & Noble, S. C. 2016, *ApJ*, 819, 48
- Sigl, G. 2012, *ArXiv e-prints*, arXiv:1202.0466
- Solomon, S. C., & Head, J. W. 1991, *Science*, 252, 252

The LIGO Scientific Collaboration, & the Virgo Collaboration. 2018, arXiv e-prints, arXiv:1811.12907

Thorne, K. S. 1994, *Black holes and time warps: Einstein’s outrageous legacy*

—. 2014, *The Science of Interstellar* (W. W. Norton & Company)

Weinberg, S. 2008, *Cosmology* (Oxford University Press)

Yang, J., Boué, G., Fabrycky, D. C., & Abbot, D. S. 2014, *ApJ*, 787, L2

Yuan, F., & Narayan, R. 2014, *ARA&A*, 52, 529

Zeldovich, Y. B., & Novikov, I. D. 1971, *Relativistic astrophysics. Vol.1: Stars and relativity*